The American Journal of Human Genetics, Volume *93*

Supplemental Data

Mutations in the Gene Encoding IFT Dynein Complex Component WDR34 Cause Jeune Asphyxiating Thoracic Dystrophy

Miriam Schmidts, Julia Vodopiutz, Sonia Christou-Savina, Claudio R. Cortés, Aideen M. McInerney-Leo, Richard D. Emes, Heleen H. Arts, Beyhan Tuysuz, Jason D'Silva, Paul J. Leo, Tom C. Giles, Machteld M. Oud, Jessica A. Harris, Marije Koopmans, Mhairi Marshall, Nursel Elçioglu, Alma Kuechler, Detlef Bockenhauer, Anthony T. Moore, Louise C. Wilson, Andreas R. Janecke, Matthew E. Hurles, Warren Emmet, Brooke Gardiner, Berthold Streubel, Belinda Dopita, Andreas Zankl, Hulya Kayserili, Peter J. Scambler, Matthew A. Brown, Philip L. Beales, Carol Wicking, UK10K Rare group, Emma L. Duncan, and Hannah M. Mitchison

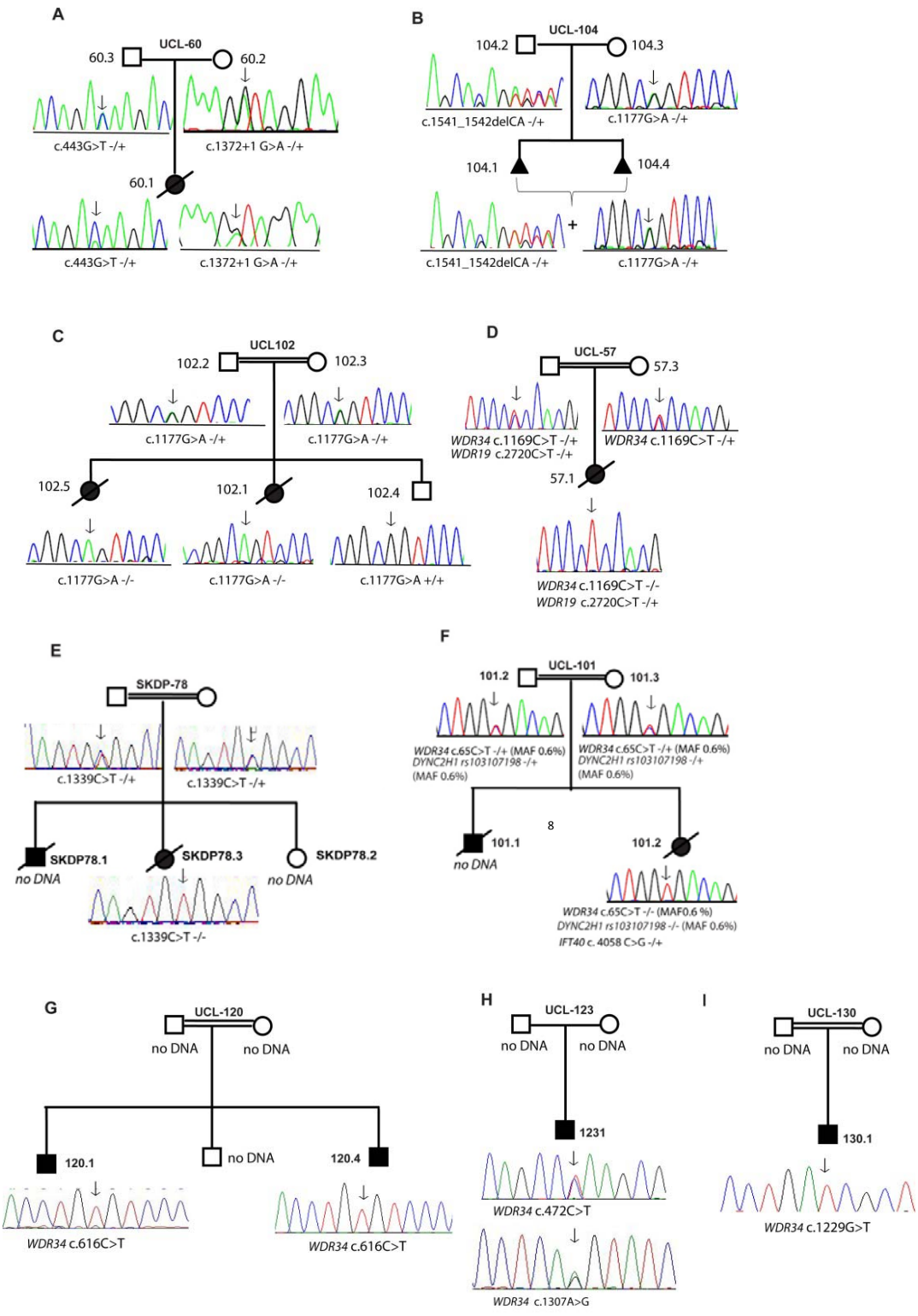

Figure S1. Segregation of *WDR34* mutations in JATD families

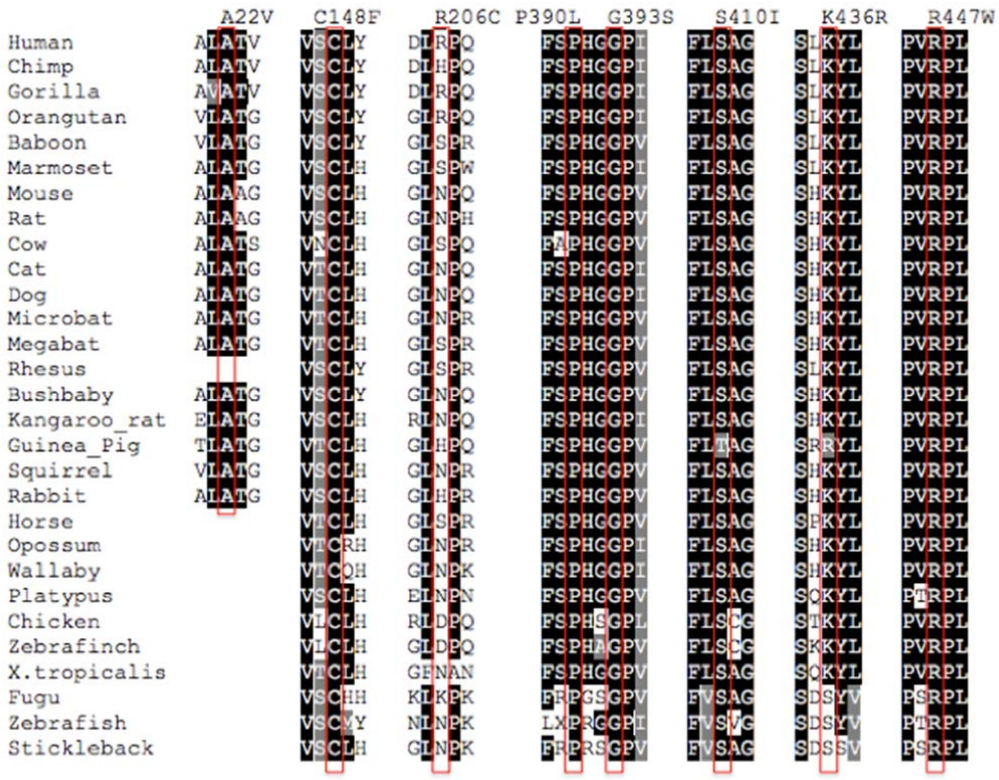

Figure S2. Cross-species conservation of amino acid residues affected by the five identified *WDR34* missense mutations

Aligned vertebrate species available from (http://hgdownload.soe.ucsc.edu/downloads.html).

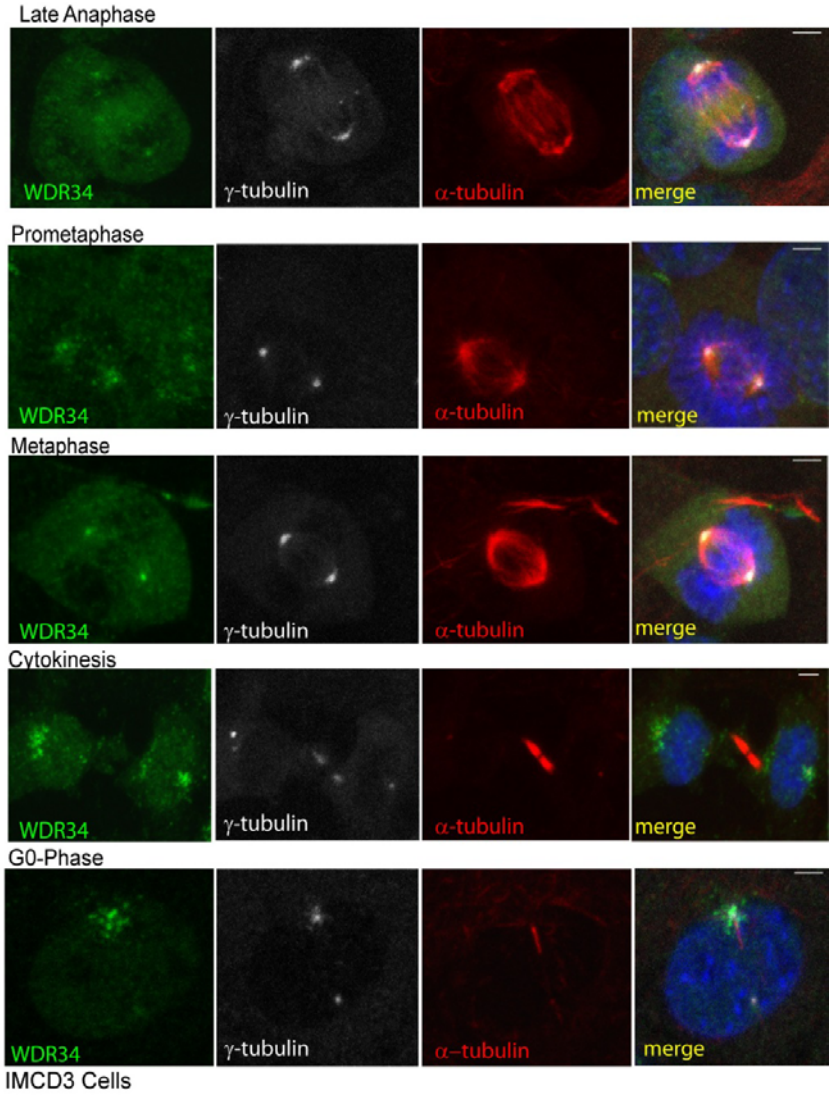

Figure S3: WDR34 localisation in IMCD3 cells during different cell cycle phases
Co-localisation of WDR34 (antibody details, green) with gamma tubulin (grey) and acetylated alpha tubulin (red) is shown during late anaphase, prometaphase, metaphase, cytokinesis and G0-phase in IMCD3 cells, counterstained with DAPI (blue). For antibody details see Figure 3.

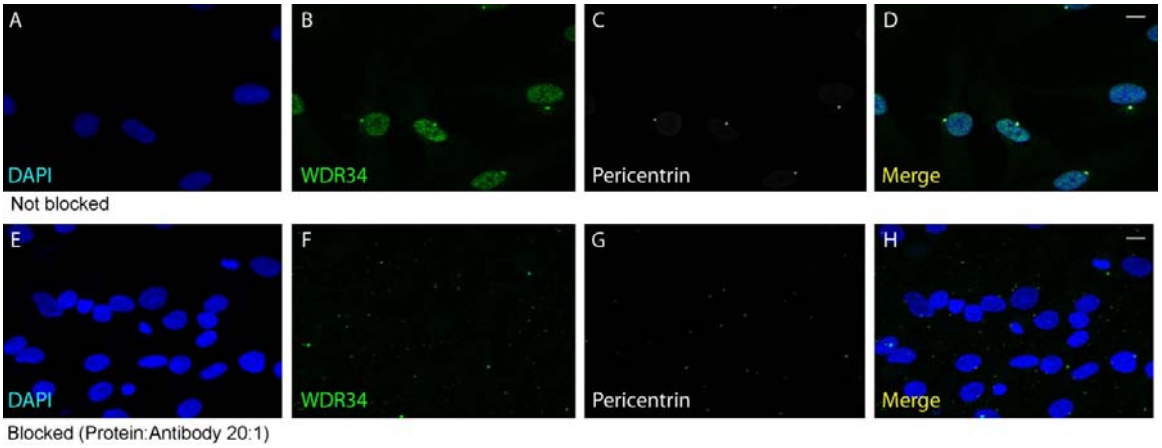

Figure S4. WDR34 antibody specificity testing by immunofluorescence
Co-localisation of WDR34 in human control fibroblasts, (green), pericentrin (grey), counterstained with DAPI (blue). WDR34 immunostaining was performed on human control fibroblasts either with (A-D) or without (E-H) pre-incubation of the WDR34 antibody with recombinant WDR34-myc protein of >80% purity (TP304288, Origene) at room temperature for 2 hours (20ng recombinant protein/ 1 ng antibody). Background staining in F does not co-localise with pericentrin (G, H), suggesting that specific WDR34 staining was competed out by the pre-incubation step. This provides support for the specificity of the WDR34 antibody. For antibody details see Figure 3.

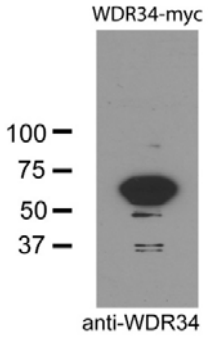

Figure S5. WDR34 antibody specificity testing in Western Blot.
500 ng of recombinant WDR34-myc protein was run on a 10% SDS gel, blotted, and the membrane was blocked for 1 hour in 5% skimmed milk powder then incubated with anti-WDR34 antibody; the secondary was an HRP-coupled anti-rabbit antibody (#7074, Cell Signaling Technology).

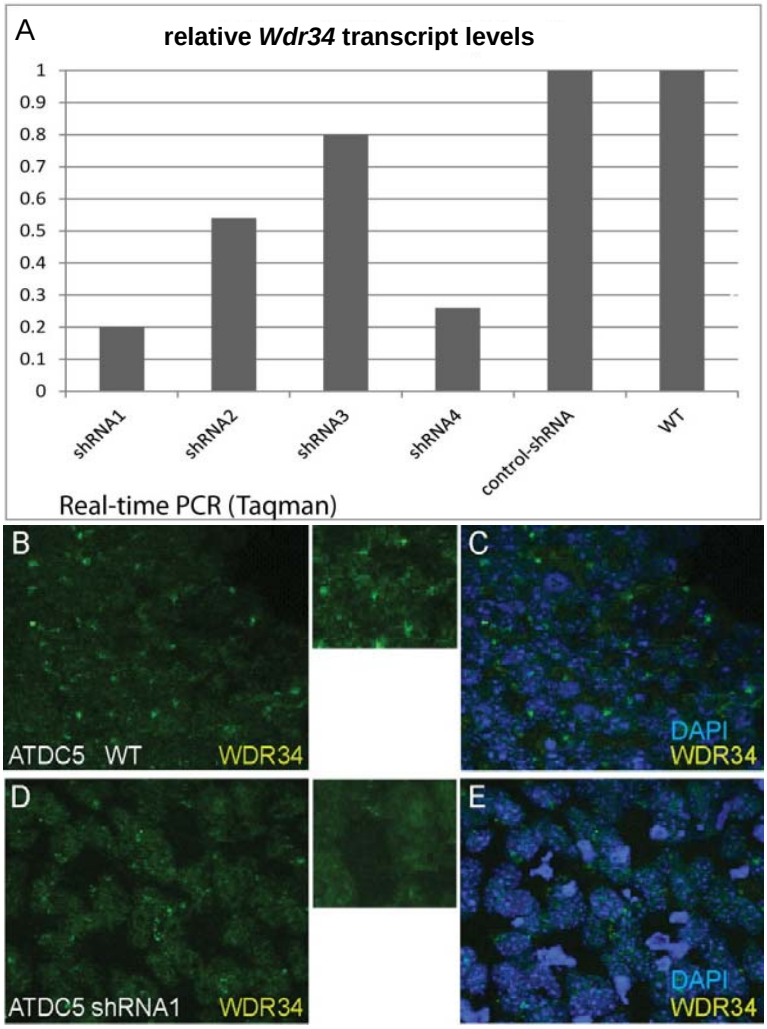

Figure S6. *Wdr34* knockdown in ATDC chondrocyte precursor cells
(A) Relative *Wdr34* transcript levels in ATDC5 cells stably transduced with *Wdr34* shRNAs 1-4, or a scrambled control shRNA are shown versus wildtype (WT) untransduced cells, assessed by real-time PCR. Knockdown of 70-80% was achieved in shRNA lines 1 and 4. RT-PCR was performed following Trizol-Chloroform RNA extraction (Invitrogen) using the Omniscript RT PCR kit (Qiagen) with a Taqman probe (*Mm*01327089_m1) for *Wdr34*, and *Wdr34* levels were normalized to GAPDH levels to compare expression levels. (B-E) Immunofluorescence analysis using anti-WDR34 antibody (green) in wildtype ATDC5 cells (top panels) or ATDC5 shRNAline 1 (bottom panels), and merged with DAPI staining (blue). Middle images are magnified from the lefthand panels to show knockdown of Wdr34 protein expression especially at the peri-basal region. Antibody details as per Figure S3.

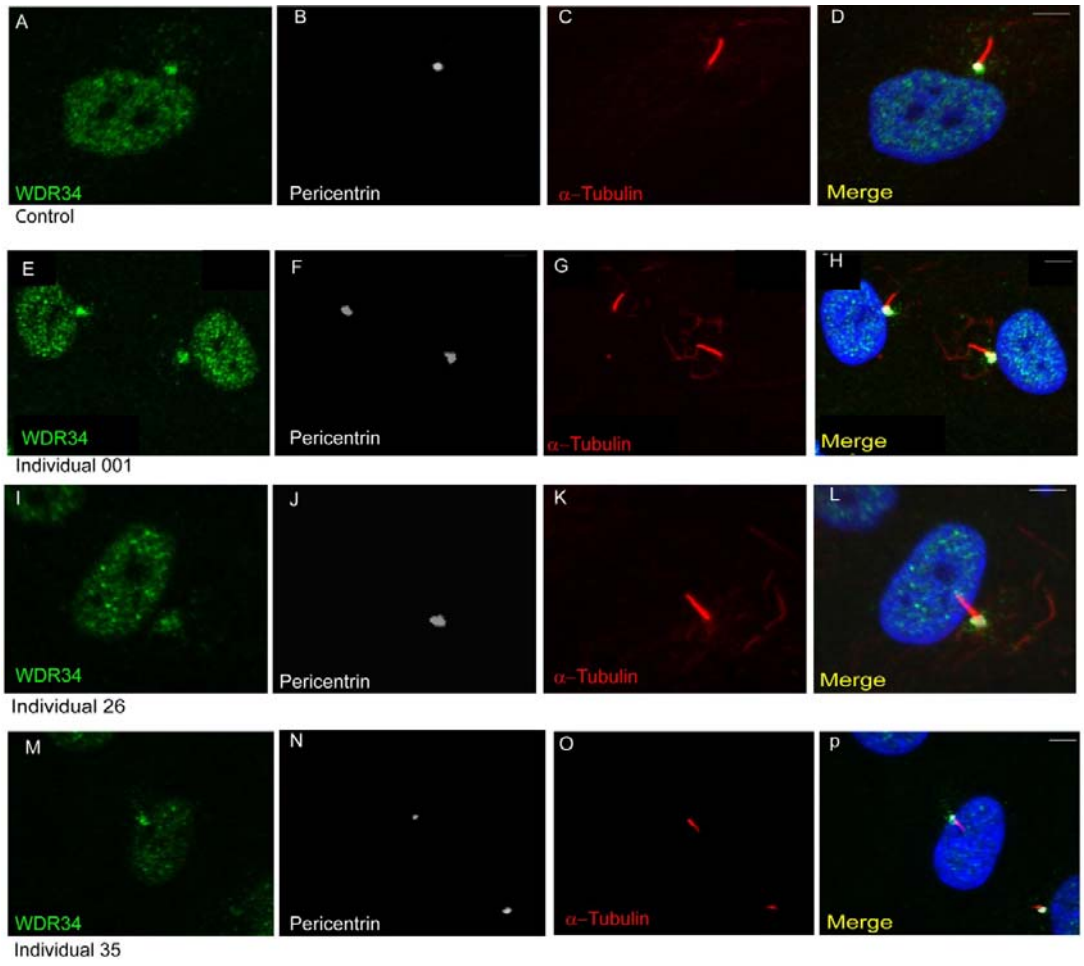

Figure S7. WDR34 localisation in *DYNC2H1*-deficient individuals with JATD and SRPS
Immunofluorescence analysis in fibroblasts of control (A-D) or Jeune patient 001 (JATD-2) carrying *DYNC2H1* homozygous missense mutation D3015G (E-H), Jeune patient 26 (JATD-3) carrying *DYNC2H1* mutations p.E3273* and p.R2481Q (I-L), and SRPS patient 35 carrying three heterozygous *DYNC2H1* mutations p.W179*, p.C291F and p.C3448P (M-P). The localisation of WDR34 (green), pericentrin (grey), acetylated tubulin (red) are shown with nuclear stain with DAPI (blue). Antibody details are the same as Figure 3.

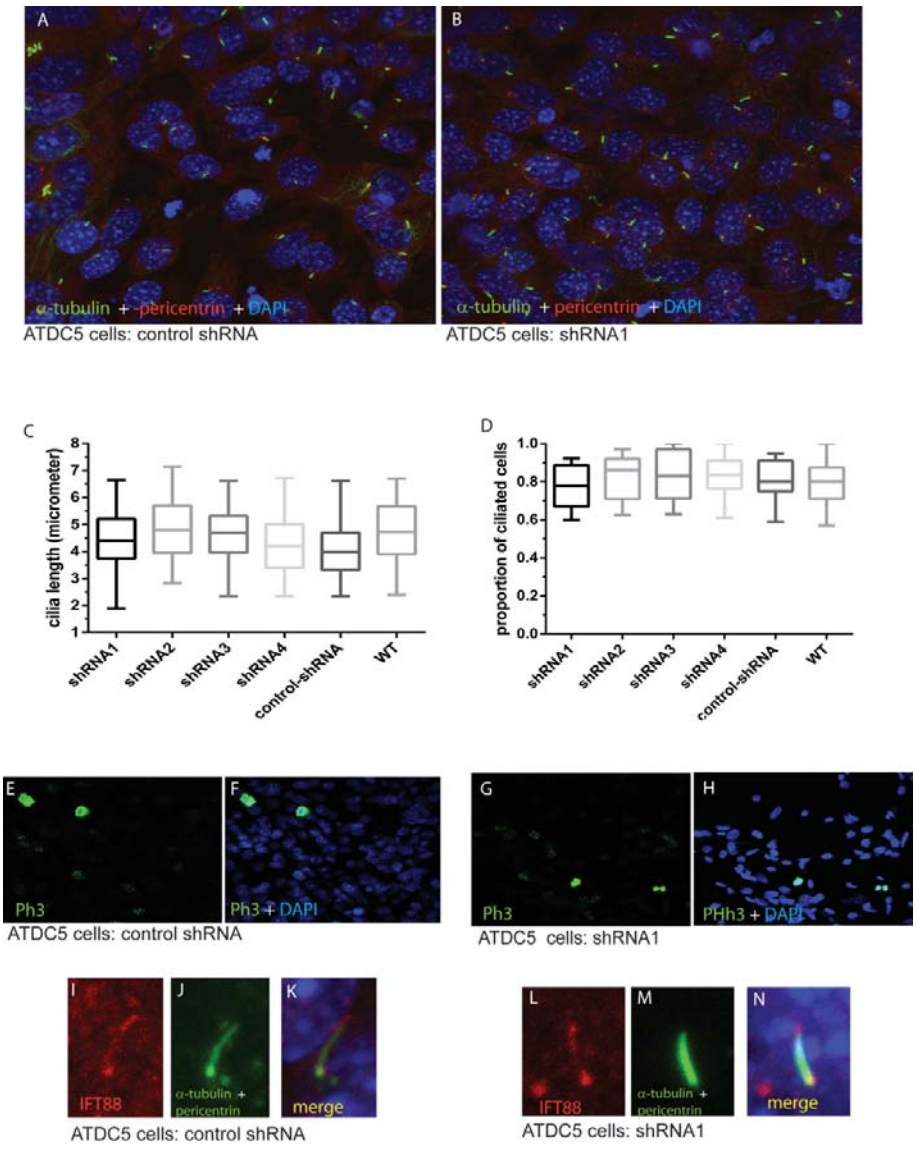

Figure S8. Ciliogenesis in *Wdr34*-knockdown ATDC5 cells

Immunofluorescence analysis of ATDC5 cells transfected with control scrambled-shRNA (A) and shRNA1 (B) using anti-WDR34 (green) and anti-pericentrin antibody (red) counterstained with DAPI (blue). shRNA line 1 (shRNA1) ATDC5 cells had 80% reduced *Wdr34* knockdown levels, as shown in Figure S7. (C) Cilia length in WT, scrambled control shRNA treated and shRNA1-4 treated ATDC5 cells after 3 days of serum starvation. (D) Proportion of ciliated WT, scrambled control-shRNA treated and shRNA1-4 treated ATDC5 cells after 3 days serum starvation. Using student's t-test analysis, the proportion of ciliated cells was averaged from 10 visual fields chosen randomly with a minimum of 25 cells per field, and cilia length estimated for a minimum 100 cells per sample. Proliferation rates in ATDC5 cells treated with control shRNA and grown under FBS supplementation visualised with anti-PH3 antibody (green, E), versus DAPI (F), in comparison to ATDC5 cells treated with shRNA1 (G, H). Localisation of IFT88 (rabbit polyclonal anti-IFT88 antibody, Proteintech) in ATDC5 cells treated with scrambled control shRNA (I K) and shRNA1 (L-N). Immunostaining as per Figure 3.

A

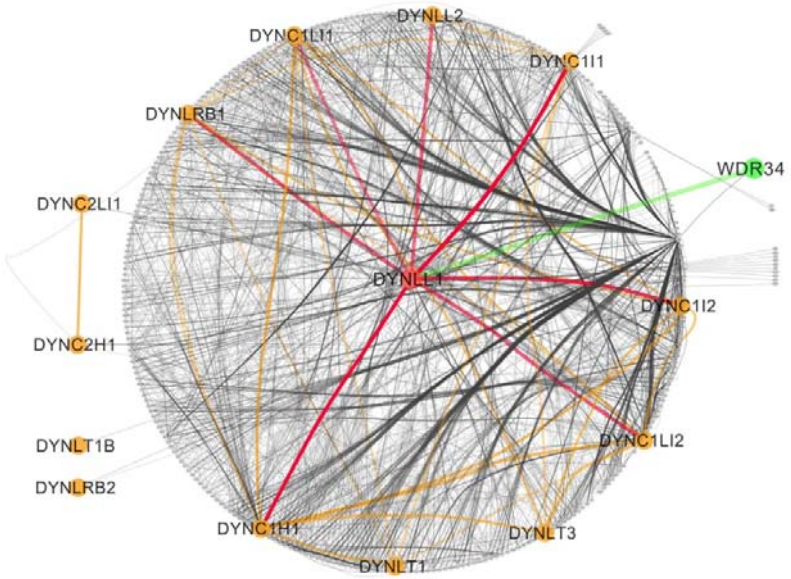

B

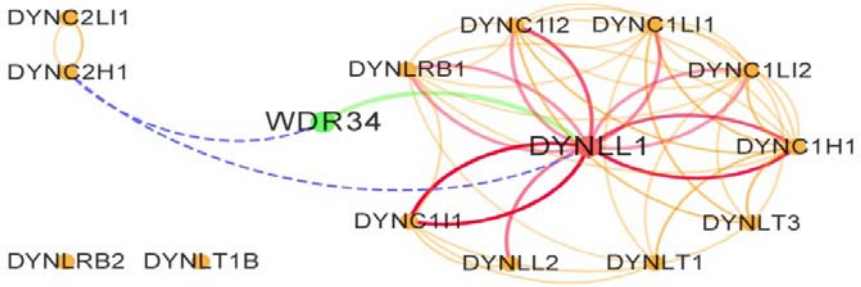

Figure S9. Potential interaction network of WDR34 and dynein-1 and dynein-2 complexes